Cite as: Y. Yanagisawa *et al.*, *Science* 10.1126/science.aam7588 (2017).

Mechanically robust, readily repairable polymers via tailored noncovalent cross-linking

Yu Yanagisawa,[1,2] Yiling Nan,[1] Kou Okuro,[1] Takuzo Aida[1,2]*

[1]Department of Chemistry and Biotechnology, School of Engineering, The University of Tokyo, 7-3-1 Hongo, Bunkyo-ku, Tokyo 113-8656, Japan. [2]RIKEN Center for Emergent Matter Science, 2-1 Hirosawa, Wako, Saitama 351-0198, Japan.

*Corresponding author. Email: aida@macro.t.u-tokyo.ac.jp

Expanding the range of healable materials is an important challenge for sustainable societies. Noncrystalline, high molecular weight polymers generally form mechanically robust materials, which, however, are difficult to repair once they are fractured. This is because their polymer chains are heavily entangled and diffuse too sluggishly to unite fractured surfaces within reasonable timescales. Here, we report that low molecular weight polymers, when cross-linked by dense hydrogen bonds, give mechanically robust yet readily repairable materials, despite their extremely slow diffusion dynamics. A key was to utilize thiourea, which anomalously forms a zigzag hydrogen-bonded array that does not induce unfavorable crystallization. Another key was to incorporate a structural element for activating the exchange of hydrogen-bonded pairs, which enables the fractured portions to rejoin readily upon compression.

Healable polymers with enhanced longevity and reliability are particularly attractive as next-generation materials for the realization of a sustainable society (*1*–*3*). On the basis of their healing mechanisms, such materials are classified as exhibiting extrinsic (*1*, *2*) or intrinsic (*1*, *3*) healing behavior. Extrinsic healing depends on the presence of finely dispersed small capsules or vascular networks that separately entrap monomers and initiators that are mixed when the containers are broken, resulting in the formation of new polymer chains that connect the fractured parts (*4*, *5*). This approach is reliable, but it allows the material to heal only a limited number of times. In contrast, intrinsic mechanisms enable polymeric materials to heal multiple times, in some cases at ambient temperatures, through the reorganization of dynamic covalent bonds (*6*–*10*) or through noncovalent interactions, mostly involving hydrogen bonds (H-bonds) (*11*–*15*). These healable materials are usually soft and deformable. Some healable materials with high mechanical properties have also been developed by cross-linking with dynamic covalent bonds. However, in most cases, heating to high temperatures, on the order of 120°C or more, to reorganize their cross-linked networks, is necessary for the fractured portions to repair (*6*–*8*).

In general, noncrystalline, high molecular weight polymers form mechanically robust materials due to the entanglement of long polymer chains. However, once the materials are fractured, they are difficult to repair unless they are heated to melt, because the entangled polymer chains diffuse too sluggishly to unite fractured portions within reasonable timescales (*2*). Meanwhile, low molecular weight polymers, when they are non-covalently cross-linked by H-bonds, may be elaborated into mechanically robust yet healable polymer materials, because their dynamic properties are modulable by changing the cross-linking density. So far, rubber-like soft materials (*11*) and thermoplastic elastomers (*14*) with H-bonding motifs have been designed to heal upon gentle compression. However, the presence of a large number of H-bonds often leads to crystallization or clustering of polymer materials, thereby making them brittle (*16*–*18*). In other words, high mechanical robustness and healing ability tend to be mutually exclusive. Here, we report that poly(ether–thioureas) such as $TUEG_2$ and $TUEG_3$ (Fig. 1A) anomalously form amorphous materials, despite carrying dense H-bonding thiourea units. More interestingly, these materials are highly robust mechanically yet can readily be repaired by compression at fractured surfaces. Why are they amorphous despite carrying a large number of H-bonded thiourea units? We found that their H-bonded thiourea arrays are geometrically nonlinear (less ordered), so that they do not induce crystallization. Originally, we prepared $TUEG_3$ as a synthetic intermediate for guanidinium ion-appended polymers that strongly bind to oxyanionic groups in biomacromolecules (*19*–*21*). During the isolation of $TUEG_3$, we noticed that cut surfaces of this polymer are self-adhesive despite their rigid and nontacky nature. In fact, cut pieces of a 2-mm-thick rectangular sheet of $TUEG_3$ (10 × 20 mm) formed a merged sheet that withstood a 300-g load, when their fractured surfaces were manually compressed for 30 s at an ambient temperature of 21°C (fig. S1).

Downloaded from http://science.sciencemag.org/ on December 14, 2017

$TUEG_3$ (Fig. 1A) can be prepared by a one-pot polycondensation of commercially available monomers (see supplementary materials; page S4). It was characterized by means of ^1H and ^{13}C NMR spectroscopy and elemental analysis. ^1H NMR end-group analysis and multiangle light-scattering studies showed that its number- and weight-average molecular weights (M_n and M_w) were 9,500 and 22,300, respectively (Fig. 1C). $TUEG_3$ is amorphous, as shown by its differential scanning calorimetry (DSC) profile on the second heating (Fig. 1B). No sharp peaks due to crystallization appeared in the temperature range from −20 to 200°C at any scan rate from 1 to 10°C/min, whereas a broad peak corresponding to a glass transition appeared at 27°C (T_g, fig. S8B). Furthermore, in its X-ray diffraction (XRD) profile recorded at 22°C, $TUEG_3$ exhibited a broad diffraction peak centered at $2\theta = 23°$, typical of an amorphous material (fig. S10B). The thiourea group is unique as a H-bonding motif (*22*), because UEG_3, the urea analog of $TUEG_3$, is semicrystalline (Fig. 1, A and B, and fig. S10E). According to a thorough crystallographic study on the geometries of H-bonded thiourea and urea derivatives (*23*), the former mostly form nonlinear zigzag arrays of H-bonded thiourea units adopting cis/trans and strained trans/trans conformations ([I] in Fig. 2A), whereas the latter form linear arrays of H-bonded urea units adopting only a trans/trans conformation ([II] in Fig. 2A). We consider that the amorphous nature of $TUEG_3$ originates from such less ordered, nonlinear geometries of its H-bonded thiourea units. Fourier-transform infrared (FTIR) spectroscopy of $TUEG_3$ at 22°C showed broad vibrational bands at around 3,290 and 3,060 cm^{-1} (Fig. 2B), the former of which can be assigned to the NH stretching vibration, while the latter is characteristic of a NH deformation vibration of nonlinearly H-bonded thiourea units (*24*). Because the estimated energy gap between the cis/trans and trans/trans conformations is 2.9–4.2 kJ/mol (*25*), these two conformers likely coexist in the polymer matrix of $TUEG_3$. Meanwhile, semicrystalline UEG_3, the urea analog of $TUEG_3$, did not display an IR absorption at around 3,060 cm^{-1} (Fig. 2B). This is in accord with a previous report that H-bonded urea units adopt only a trans/trans conformation (Fig. 2, A and B) (*23*). The contrasting FTIR spectral features observed for amorphous $TUEG_3$ and semicrystalline UEG_3 highlight an important principle that densely located thiourea units, like urea units, tightly cross-link the polymer main chains through H-bonding interactions but do not induce crystallization because the resultant H-bonded arrays are nonlinear and less ordered.

To follow up on our preliminary healing test of $TUEG_3$ described above (fig. S1), we fabricated tensile bars by a method analogous to that used for the preparation of the polymer sheet, and then subjected the bars to tensile tests (test rate: 10 mm/min) at an ambient temperature of 21°C. The stress–strain curve, shown in Fig. 1D (red solid curve), displayed an abrupt increase in stress of as much as 45 ± 8 MPa, and the sample yielded at an applied strain of 6 ± 2%. After this yielding stage, the specimen elongated by up to 393 ± 5% before fracture (fig. S11). The elastic modulus of $TUEG_3$, as estimated from the initial slope of the stress–strain curve (Fig. 1D), was 1.4 GPa. Since dynamic mechanical properties are important for understanding the healing events at fractured portions, we performed temperature-dispersion tests for $TUEG_3$ at 200–0°C (5°C/min) at a constant frequency (ω) of 10 rad/s. The storage modulus (G') and loss modulus (G'') curves of $TUEG_3$ allowed for confirming the glass transition at around 30°C (fig. S12B). Noteworthy, $TUEG_3$ displayed a rubber plateau region, typical of long polymer chains upon being entangled, at around 50–70°C, despite the fact that its molecular weight is less than 10 kDa.

We then tested the healing of $TUEG_3$ by a method analogous to that reported by Corté and co-workers (*26*). Thus, a 0.1-mm-thick sheet of Teflon (10 × 10 mm) with a 1-mm-diameter hole at its center (Fig. 3A) was sandwiched between two discs of $TUEG_3$ (diameter: 8 mm; thickness: 1.0 mm). This assembled specimen was set on a rheometer stage, gently pressed with a jig, and then annealed for 20 min at 90°C (hot melt), so that the touching parts of the upper and lower discs merged inside the hole area of the Teflon sheet. The resultant specimen was cooled to 24°C at a rate of 5°C/min, and then the stage and jig in the rheometer were rapidly separated from one another at a rate of 100 mm/min to cause brittle fracture in the merged part of the specimen. After 3 min, the fractured surfaces were mechanically brought back into contact and compressed at the designated temperature under a constant applied stress. The compressed specimen was then subjected to tensile testing (tensile rate: 2 mm/min) to determine the stress at fracture. Although the contact area between the upper and lower discs was only 0.79 mm^2, the tensile tests were highly reproducible (fig. S13). Even when the contact area was enlarged from 0.79 to 1.76, 3.14, or 19.6 mm^2 (figs. S14 and S15), the results obtained were consistent (fig. S16). Meanwhile, when the applied compression stress was increased from 0.12 to 1.0 MPa, the recovery levelled off at 0.4 MPa after the initial abrupt increase (fig. S17). On the basis of these results, we carried out systematic healing tests by setting the contact area and applied compression stress at 0.79 mm^2 and 1.0 MPa, respectively. Figure 3B shows the stresses at break (black circles) observed for the assembled specimens of $TUEG_3$ prepared by compression for 1 hour at various temperatures (T_{comp} = 10–36°C). Note that the elastic moduli (red circles) of the compressed specimens at ≤ 32°C were rather high (≥ 0.9 GPa). Figure 3D shows the percentage recoveries of the stresses at break ($\sigma/\sigma_{pristine} \times 100$) of $TUEG_3$, where the specimen compressed at 24°C completely recovered its original mechanical strength ($\sigma_{pristine}$) in 6 hours. Accordingly, the interfacial adhesion energy was estimated to

Downloaded from http://science.sciencemag.org/ on December 14, 2017

be ~0.9 J/m^2 (supplementary materials; page S4). When T_{comp} was raised from 24°C to the higher range of 28–36°C, the specimen completely recovered within 1 hour (Fig. 3B), and the healing could be repeated multiple times without noticeable deterioration (fig. S18). Notably, even at T_{comp} = 12°C, the specimen recovered partially. On the basis of the frequency-dispersion properties of the G' and G'' values at 20–100°C with ω = 628 to 6.28 × 10^{-3} rad/s (figs. S19 and S20), we estimated the relaxation times (τ) for the flow transition of $TUEG_3$ by using their master curves (*27*) at 24–32°C (Fig. 3E and fig. S21). The τ values were in the range 10^7 seconds (~months) to 10^5 seconds (~days) (Fig. 3F), which are far longer than the compression times required for $TUEG_3$ to heal completely at T_{comp} = 24–32°C (≤ 6 hours). This contrast suggests that the rapid healing behavior of $TUEG_3$ is not a consequence of the flow of polymer chains (*11*, *14*), but is certainly dominated by a much more rapid process.

Other polymeric thiourea derivatives $TUEG_2$, $TUEG_4$, TUC_8, and TUC_{12} (Fig. 1A), in which diethylene glycol, tetraethylene glycol, octamethylene, and dodecamethylene spacer units, respectively, connect the thiourea units, were synthesized. Just like $TUEG_3$, $TUEG_2$ and $TUEG_4$ were both amorphous and displayed only single broad glass-transition peaks at 58 and 5°C, respectively (Fig. 1B and figs. S8 and S10). TUC_8 was also amorphous (T_g = 39°C), whereas TUC_{12} was semicrystalline (Fig. 1B and figs. S8 and S10). As in the case of $TUEG_3$, the FTIR spectra (Fig. 2B) of these reference polymers exhibited NH stretching and deformation vibrations in a range of 3,250–3,300 cm^{-1} and at around 3,060 cm^{-1}, respectively, the latter of which is typical of nonlinear H-bonded arrays of thiourea units (*23*). We investigated the tensile behaviors of these polymers and that of UEG_3 at an ambient temperature of 21°C with a tensile rate of 10 mm/min (Fig. 1D). In contrast to $TUEG_3$, all of these polymers were highly brittle, except $TUEG_4$ that was too fluid-like to be tested. However, in the tensile tests just below their glass transition temperatures, $TUEG_2$ did not fracture in a brittle manner, but yielded like $TUEG_3$, whereas TUC_8 again showed brittle fracture (fig. S23). We then conducted healing tests on amorphous $TUEG_2$ and TUC_8 at T_{comp} = 58 and 44°C, respectively. These temperatures were employed in order to properly compare the healing behaviors of these polymers with those of $TUEG_3$ at 24°C (Fig. 3D), since their viscosities, as determined by shear creep tests, were in the same level as one another (2.5 × 10^9 Pa·s for $TUEG_2$ at 58°C, 2.2 × 10^9 Pa·s for TUC_8 at 44°C, and 3.3 × 10^9 Pa·s for $TUEG_3$ at 24°C) (fig. S25). Figure 3D shows that $TUEG_2$ at T_{comp} = 58°C displayed an 85% recovery of its mechanical strength ($\sigma_{pristine}$) upon compression for 6 hours. Even when T_{comp} was lowered to 48°C (Fig. 3C, black circles), compressed $TUEG_2$ showed a partial recovery (22%) in 1 hour, although the elastic modulus of $TUEG_2$, at temperatures up to 70°C, remained high (≥ 1 GPa) (Fig. 3C, red circles). In contrast, TUC_8 barely healed, even upon compression at 44°C over a long period of 24 hours. Analogous to the case of $TUEG_3$, we evaluated the relaxation times (τ) of $TUEG_2$ and TUC_8 for the flow transition (fig. S22) from their temperature-dispersion (fig. S12) and frequency-dispersion properties (figs. S19 and S20). As shown in fig. S22, $TUEG_2$ and TUC_8 displayed a rubber plateau region similar to that of $TUEG_3$. Furthermore, both of these polymers showed extremely slow relaxation properties at T_{comp} [τ = 10^7 s (~months) to 10^6 s (~weeks)]. Why can $TUEG_2$ as well as $TUEG_3$ readily heal despite such slow diffusion dynamics? We consider that their healing properties are dominated by a segmental motion such as the exchange of H-bonded thiourea pairs, leading to the interpenetration of polymer chains at the fractured portions upon compression (*28*). The H-bond exchange of thiourea pairs should occur far more rapidly than the flow relaxation of these polymers (Fig. 3E and figs. S21 and S22). Consequently, virtually frozen $TUEG_2$ and $TUEG_3$ can heal only in a few hours. Then, why does TUC_8 hardly heal? This question prompted us to consider a special role of the spacer units that connect the thiourea units. Arrhenius plots of the intersection frequencies for the storage modulus (G') and loss modulus (G'') curves (fig. S20) allowed us to estimate the apparent activation energies (E_a) for the slippage of polymer chains (Fig. 4A). As shown in Fig. 4B, the E_a values for $TUEG_2$, $TUEG_3$, and TUC_8 were 171, 149, and 203 kJ/mol, respectively. In H-bonded polymer materials, polymer chains presumably slip and interpenetrate by exchanging their H-bonded pairs. According to the Flory–Huggins interaction parameters (χ) of the model structures in Fig. 4C, thiourea is much more miscible with ethers than with hydrocarbons. In ethereal media, the ether oxygen atoms might facilitate the exchange of H-bonded thiourea pairs by serving as temporal H-bond acceptors (Fig. 4D); in other words, the ether-containing $TUEG_2$ and $TUEG_3$ utilize this mechanism to lower the energy barrier for the slippage of their polymer chains. Obviously, this is not the case in TUC_8, since the thiourea group is incompatible with hydrocarbons (Fig. 4C). It is therefore reasonable that the E_a value for TUC_8 is larger than those for ether-containing $TUEG_2$ and $TUEG_3$, and the same might hold true even in a lower temperature range.

The present work provides the essential structural elements listed below for the design of mechanically robust yet healable polymer materials: (1) relatively short polymer chains that permit greater segmental motions, (2) tight cross-links by a large number of H-bonds for better mechanical properties, (3) nonlinear (less ordered) H-bond arrays that do not induce crystallization, and (4) implemented mechanisms to facilitate the exchange of H-bonded pairs. The triethylene glycol spacer that connects the thiourea units in $TUEG_3$ optimally modulates the activation energy for the exchange of H-

Downloaded from http://science.sciencemag.org/ on December 14, 2017

bonded thiourea pairs; consequently, the polymer material, although highly cross-linked noncovalently, can heal by only compression without heating.

REFERENCES AND NOTES

1. C. E. Diesendruck, N. R. Sottos, J. S. Moore, S. R. White, Biomimetic self-healing. *Angew. Chem. Int. Ed.* **54**, 10428–10447 (2015). doi:10.1002/anie.201500484 Medline
2. R. P. Wool, Self-healing materials: A review. *Soft Matter* **4**, 400–418 (2008). doi:10.1039/b711716g
3. Y. Yang, M. W. Urban, Self-healing polymeric materials. *Chem. Soc. Rev.* **42**, 7446–7467 (2013). doi:10.1039/c3cs60109a Medline
4. S. R. White, N. R. Sottos, P. H. Geubelle, J. S. Moore, M. R. Kessler, S. R. Sriram, E. N. Brown, S. Viswanathan, Autonomic healing of polymer composites. *Nature* **409**, 794–797 (2001). doi:10.1038/35057232 Medline
5. K. S. Toohey, N. R. Sottos, J. A. Lewis, J. S. Moore, S. R. White, Self-healing materials with microvascular networks. *Nat. Mater.* **6**, 581–585 (2007). doi:10.1038/nmat1934 Medline
6. X. Chen, M. A. Dam, K. Ono, A. Mal, H. Shen, S. R. Nutt, K. Sheran, F. Wudl, A thermally re-mendable cross-linked polymeric material. *Science* **295**, 1698–1702 (2002). doi:10.1126/science.1065879 Medline
7. D. Montarnal, M. Capelot, F. Tournilhac, L. Leibler, Silica-like malleable materials from permanent organic networks. *Science* **334**, 965–968 (2011). doi:10.1126/science.1212648 Medline
8. J. P. Brutman, P. A. Delgado, M. A. Hillmyer, Polylactide vitrimers. *ACS Macro Lett.* **3**, 607–610 (2014). doi:10.1021/mz500269w
9. M. Capelot, D. Montarnal, F. Tournilhac, L. Leibler, Metal-catalyzed transesterification for healing and assembling of thermosets. *J. Am. Chem. Soc.* **134**, 7664–7667 (2012). doi:10.1021/ja302894k Medline
10. Y. Yang, Z. Pei, X. Zhang, L. Tao, Y. Wei, Y. Ji, Carbon nanotube–vitrimer composite for facile and efficient photo-welding of epoxy. *Chem. Sci.* **5**, 3486–3492 (2014). doi:10.1039/C4SC00543K
11. P. Cordier, F. Tournilhac, C. Soulié-Ziakovic, L. Leibler, Self-healing and thermoreversible rubber from supramolecular assembly. *Nature* **451**, 977–980 (2008). doi:10.1038/nature06669 Medline
12. A. M. Kushner, J. D. Vossler, G. A. Williams, Z. Guan, A biomimetic modular polymer with tough and adaptive properties. *J. Am. Chem. Soc.* **131**, 8766–8768 (2009). doi:10.1021/ja9009666 Medline
13. J. Fox, J. J. Wie, B. W. Greenland, S. Burattini, W. Hayes, H. M. Colquhoun, M. E. Mackay, S. J. Rowan, High-strength, healable, supramolecular polymer nanocomposites. *J. Am. Chem. Soc.* **134**, 5362–5368 (2012). doi:10.1021/ja300050x Medline
14. Y. Chen, A. M. Kushner, G. A. Williams, Z. Guan, Multiphase design of autonomic self-healing thermoplastic elastomers. *Nat. Chem.* **4**, 467–472 (2012). doi:10.1038/nchem.1314 Medline
15. T. L. Sun, T. Kurokawa, S. Kuroda, A. B. Ihsan, T. Akasaki, K. Sato, M. A. Haque, T. Nakajima, J. P. Gong, Physical hydrogels composed of polyampholytes demonstrate high toughness and viscoelasticity. *Nat. Mater.* **12**, 932–937 (2013). doi:10.1038/nmat3713 Medline
16. D. Boils, M.-È. Perron, F. Monchamp, H. Duval, T. Maris, J. D. Wuest, Molecular tectonics. Disruption of self-association in melts derived from hydrogen-bonded solids. *Macromolecules* **37**, 7351–7357 (2004). doi:10.1021/ma035977d
17. O. Lebel, T. Maris, M.-È. Perron, E. Demers, J. D. Wuest, The dark side of crystal engineering: Creating glasses from small symmetric molecules that form multiple hydrogen bonds. *J. Am. Chem. Soc.* **128**, 10372–10373 (2006). doi:10.1021/ja063353s Medline
18. C. B. St.Pourcain, A. C. Griffin, Thermoreversible supramolecular networks with polymeric properties. *Macromolecules* **28**, 4116–4121 (1995). doi:10.1021/ma00116a010
19. R. Mogaki, K. Okuro, T. Aida, Molecular glues for manipulating enzymes: Trypsin inhibition by benzamidine-conjugated molecular glues. *Chem. Sci.* **6**, 2802–2805 (2015). doi:10.1039/C5SC00524H Medline
20. P. K. Hashim, K. Okuro, S. Sasaki, Y. Hoashi, T. Aida, Reductively cleavable nanocaplets for siRNA delivery by template-assisted oxidative polymerization. *J. Am. Chem. Soc.* **137**, 15608–15611 (2015). doi:10.1021/jacs.5b08948 Medline
21. R. Mogaki, P. K. Hashim, K. Okuro, T. Aida, Guanidinium-based "molecular glues" for modulation of biomolecular functions. *Chem. Soc. Rev.* **46**, 6480–6491 (2017). doi:10.1039/C7CS00647K Medline
22. C. Stefaniu, P.-L. Zaffalon, A. Carmine, Q. Verolet, S. Fernandez, T. A. Wesolowski, G. Brezesinski, A. Zumbuehl, Rigid urea and self-healing thiourea ethanolamine monolayers. *Langmuir* **31**, 1296–1302 (2015). doi:10.1021/la5039987 Medline
23. R. Custelcean, Crystal engineering with urea and thiourea hydrogen-bonding groups. *Chem. Commun.* **2008**, 295–307 (2008). doi:10.1039/B708921J Medline
24. R. Custelcean, M. G. Gorbunova, P. V. Bonnesen, Steric control over hydrogen bonding in crystalline organic solids: A structural study of *N,N'*-dialkylthioureas. *Chemistry* **11**, 1459–1466 (2005). doi:10.1002/chem.200400973 Medline
25. M. Obrzud, M. Rospenk, A. Koll, Self-association of N,N'-dialkylthiourea derivatives in non-polar solvents. *J. Mol. Struct.* **1018**, 54–63 (2012). doi:10.1016/j.molstruc.2012.01.042
26. F. Maes, D. Montarnal, S. Cantournet, F. Tournilhac, L. Corté, L. Leibler, Activation and deactivation of self-healing in supramolecular rubbers. *Soft Matter* **8**, 1681–1687 (2012). doi:10.1039/C2SM06715C
27. M. Rubinstein, R. H. Colby, *Polymer Physics* (Oxford Univ. Press, 2003).
28. S. Seiffert, J. Sprakel, Physical chemistry of supramolecular polymer networks. *Chem. Soc. Rev.* **41**, 909–930 (2012). doi:10.1039/C1CS15191F Medline
29. R. F. Fedors, A method for estimating both the solubility parameters and molar volumes of liquids. *Polym. Eng. Sci.* **14**, 147–154 (1974). doi:10.1002/pen.760140211
30. J. Brandrup, E. H. Immergut, E. A. Grulke (Eds.), *Polymer Handbook* (Wiley, ed. 4, 2003).
31. P. G. de Gennes, Soft adhesives. *Langmuir* **12**, 4497–4500 (1996). doi:10.1021/la950886y

ACKNOWLEDGMENTS

We appreciate the valuable discussion provided by Professors Z. Guan (University of California, Irvine), K. Mayumi, and K. Ito (The University of Tokyo), and Dr. H. Sasaki (Toagosei Co. Ltd.) and Dr. E. Silver and Mr. K. Morishita (The University of Tokyo). We also thank Professors H. Ejima and N. Yoshie (The University of Tokyo), and Messrs. Y. Kamei, H. Ochiai, and A. Masumoto (Shimadzu Corporation) for performing the mechanical tests, and Ms. M. Ishikawa (Tokyo Institute of Technology), Messrs. M. Nakamura, K. Kurono, and Dr. T. Tokai (Shoko Science Co. Ltd.) for the MALS analysis. This work was financially supported by a Grant-in-Aid for Specially Promoted Research (25000005) on 'Physically Perturbed Assembly for Tailoring High-Performance Soft Materials with Controlled Macroscopic Structural Anisotropy'. We also acknowledge assistance from the ImPACT Program of the Council for Science, Technology and Innovation (Cabinet Office, Government of Japan). Y.Y. thanks the Fellowship of Japan Society for the Promotion of Science (JSPS) for Young Scientists and the Program for Leading Graduate Schools (MERIT).

SUPPLEMENTARY MATERIALS

www.sciencemag.org/cgi/content/full/science.aam7588/DC1
Materials and Methods
Figs. S1 to S25
Reference (*31*)
Movie S1

12 January 2017; accepted 4 December 2017
Published online 14 December 2017
10.1126/science.aam7588

Downloaded from http://science.sciencemag.org/ on December 14, 2017

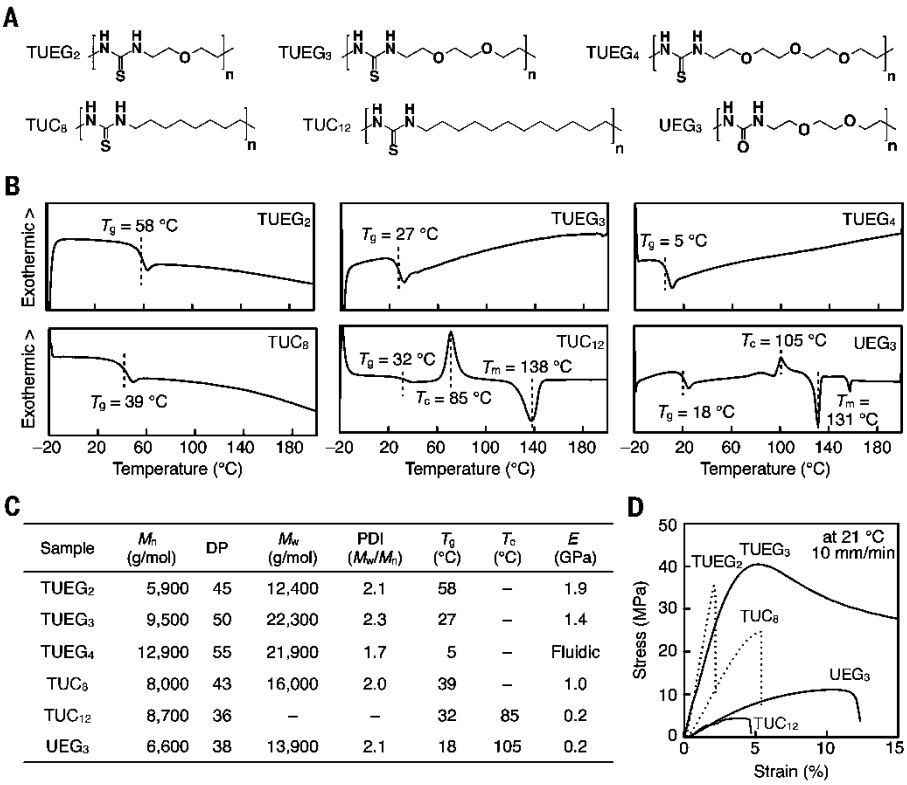

Sample	M_n (g/mol)	DP	M_w (g/mol)	PDI (M_w/M_n)	T_g (°C)	T_c (°C)	E (GPa)
$TUEG_2$	5,900	45	12,400	2.1	58	–	1.9
$TUEG_3$	9,500	50	22,300	2.3	27	–	1.4
$TUEG_4$	12,900	55	21,900	1.7	5	–	Fluidic
TUC_8	8,000	43	16,000	2.0	39	–	1.0
TUC_{12}	8,700	36	–	–	32	85	0.2
UEG_3	6,600	38	13,900	2.1	18	105	0.2

Fig. 1. **Molecular structures and characterization of poly(ether-thiourea) $TUEG_3$ and its reference polymers.** (**A**) Schematic structures of poly(ether-thioureas) with diethylene glycol ($TUEG_2$), triethylene glycol ($TUEG_3$), and tetraethylene glycol ($TUEG_4$) as spacers; schematic structures of poly(alkylene-thioureas) with octamethylene (TUC_8) and dodecamethylene chains (TUC_{12}) as spacers, and schematic structure of a poly(ether-urea) with triethylene glycol (UEG_3) as a spacer. (**B**) Differential scanning calorimetry (DSC) thermograms for $TUEG_2$, $TUEG_3$, $TUEG_4$, TUC_8, TUC_{12}, and UEG_3 on the second heating from −20°C to 200°C at a rate of 10°C/min. T_g, T_c, and T_m denote the glass-transition temperature, crystallization temperature, and melting temperature, respectively. (**C**) Characterization of polymers. M_n is the number-average molecular weight and DP is the degree of polymerization as estimated by ^{1}H NMR end-group analysis, M_w is the weight-average molecular weight, obtained by multiangle light scattering, and PDI is the polydispersity index (M_w/M_n); E is the elastic modulus, evaluated from the stress–strain curve in tensile testing (Fig. 1D); (**D**) Stress–strain curves of $TUEG_2$, $TUEG_3$, TUC_8, TUC_{12}, and UEG_3 at 21°C.

Downloaded from http://science.sciencemag.org/ on December 14, 2017

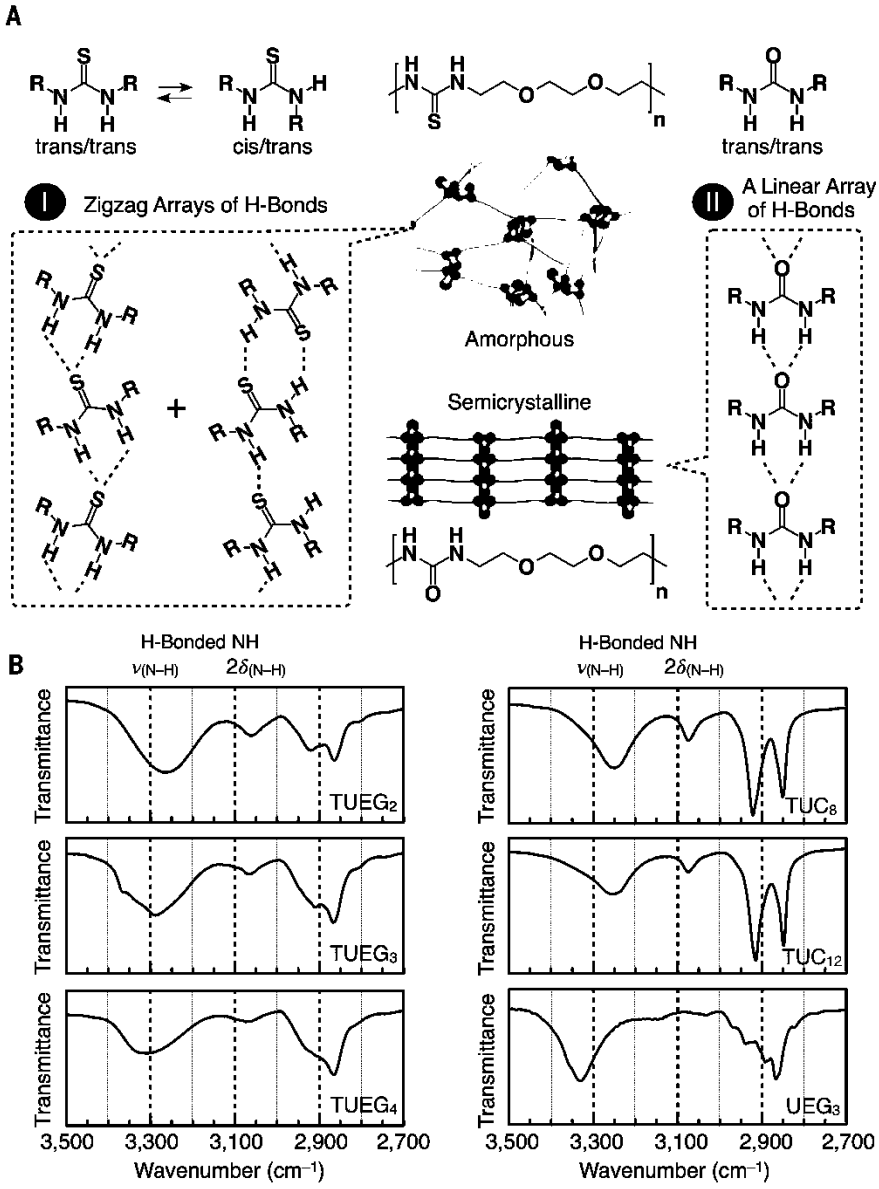

Fig. 2. Hydrogen-bonding interactions of thiourea and urea moieties in polymer matrices. (A) Schematic representations of the hydrogen-bonding modes of thiourea and urea. (B) FTIR spectra (bulk) at 22°C of poly(ether-thioureas) $TUEG_2$, $TUEG_3$, and $TUEG_4$; poly(alkylene-thioureas) TUC_8 and TUC_{12}; and poly(ether-urea) UEG_3.

Downloaded from http://science.sciencemag.org/ on December 14, 2017

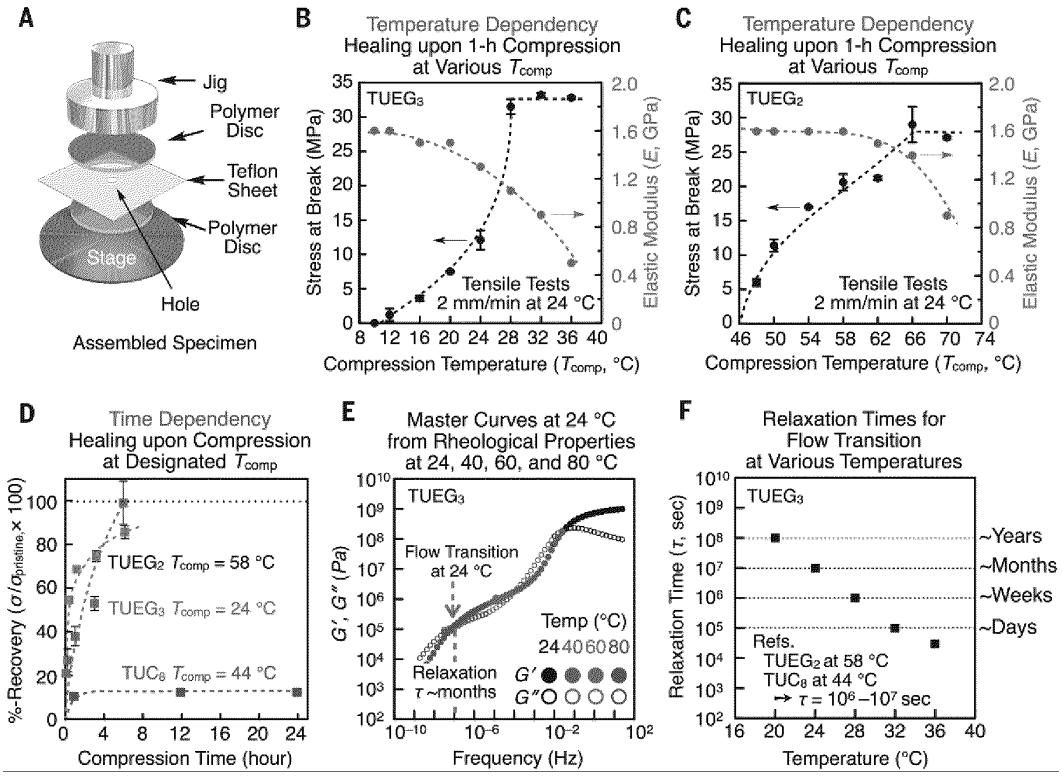

Fig. 3. Healing behaviors of polymeric thiourea derivatives upon compression. (A to D) Healing tests using a rheometer (*26*): (A) Schematic representation of the assembled specimen. (B and C) Elastic moduli (E, red circles) of poly(ether-thioureas) (B) $TUEG_3$ and (C) $TUEG_2$ at various temperatures, as estimated by compression testing (10 mm/min; red circles), and stresses at break for the assembled specimens (black circles) prepared by compression for 1 hour at various temperatures under a constant applied stress of 1.0 MPa. (D) Percentage recoveries of the stress at break for assembled specimens of $TUEG_2$, $TUEG_3$, and TUC_8 ($\sigma_{pristine}$; 26.5 ± 0.3, 31.7 ± 0.5, 39.1 ± 1.6 MPa, respectively), prepared by compression for various periods of time at T_{comp} of 58, 24, and 44°C, respectively, under a constant applied stress of 1.0 MPa. (E) Master curves for $TUEG_3$ at a reference temperature of 24°C, prepared by the time–temperature superposition treatment of G' and G'' values obtained at 24, 40, 60, and 80°C in frequency (ω)-dispersion tests at $\omega = 628$ to 6.28×10^{-3} rad/s at an applied strain of 0.05 or 0.1%. (F) Relaxation times (τ) of $TUEG_3$ for the flow transition, estimated from the crossover points of G' and G'' at various temperatures (20–36°C) (fig. S21).

Downloaded from http://science.sciencemag.org/ on December 14, 2017

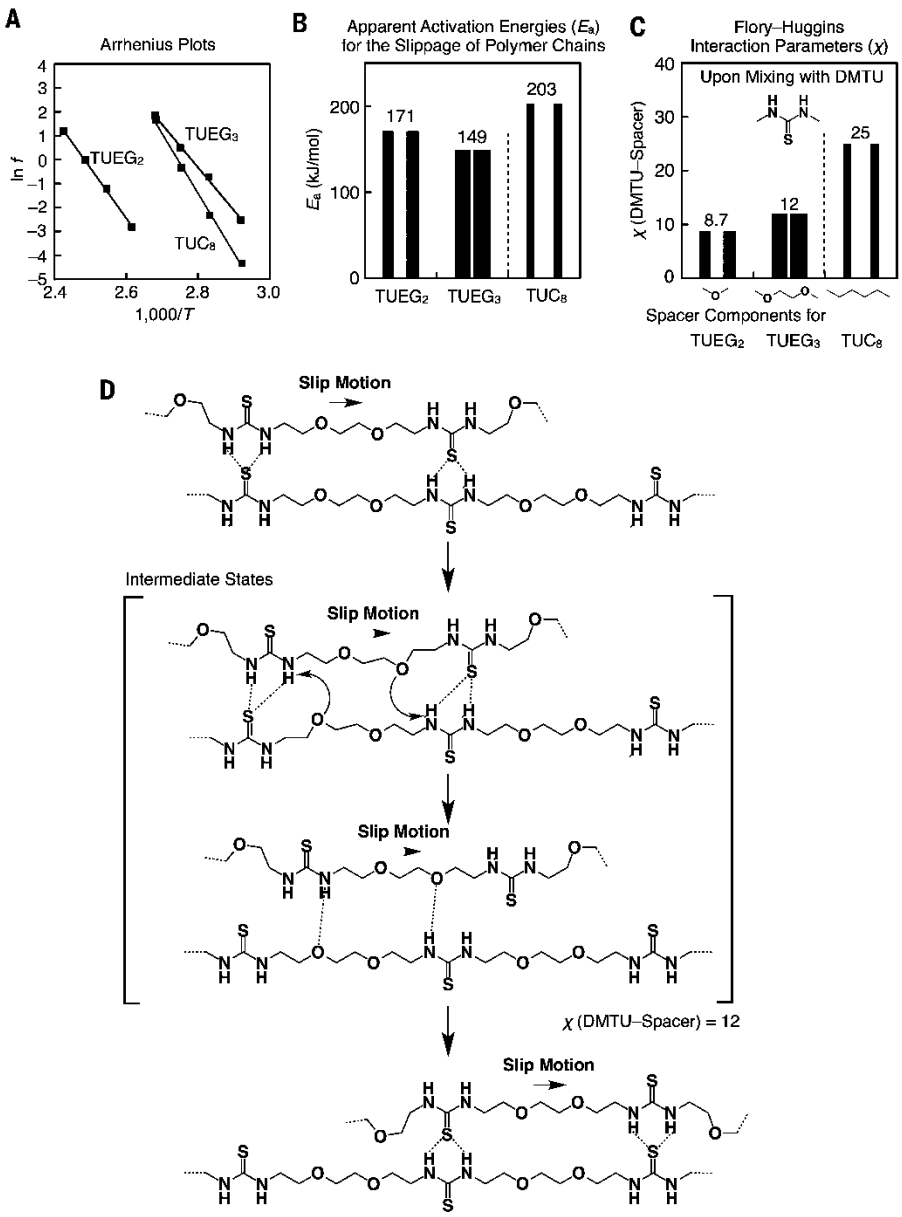

Fig. 4. Slip motions of polymer chains in poly(ether-thiourea) and poly(alkylene-thiourea) through exchange of hydrogen-bonded pairs. (**A**) Arrhenius plots of the intersection frequencies for the storage-modulus (G') and 1oss-modulus (G'') curves of poly(ether-thioureas) $TUEG_2$ and $TUEG_3$ and poly(alkylene-thiourea) TUC_8, estimated from a frequency (ω) sweep tests at ω = 100–0.05 rad/s at a constant applied strain of 0.1% in the temperature range for the flow transition (fig. S20). (**B**) Apparent activation energies (E_a) of $TUEG_2$, $TUEG_3$, and TUC_8 for the slippage of polymer chains, estimated from the Arrhenius plots. (**C**) Flory–Huggins interaction parameters χ (DMTU–Spacer) for *N*,*N'*-dimethylthiourea (DMTU) in combination with dimethyl ether (a model mixture for $TUEG_2$), ethylene glycol dimethyl ether (a model mixture for $TUEG_3$), or hexane (a model mixture for TUC_8). These values were estimated from the corresponding Hildebrand solubility parameters, determined by the Fedors method (*29*, *30*). (**D**) Proposed mechanism of how the exchange of H-bonded thiourea pairs in $TUEG_3$ is enhanced.

Downloaded from http://science.sciencemag.org/ on December 14, 2017

Science

Mechanically robust, readily repairable polymers via tailored noncovalent cross-linking

Yu Yanagisawa, Yiling Nan, Kou Okuro and Takuzo Aida

published online December 14, 2017

ARTICLE TOOLS http://science.sciencemag.org/content/early/2017/12/13/science.aam7588

SUPPLEMENTARY MATERIALS http://science.sciencemag.org/content/suppl/2017/12/13/science.aam7588.DC1

REFERENCES This article cites 29 articles, 2 of which you can access for free
http://science.sciencemag.org/content/early/2017/12/13/science.aam7588#BIBL

PERMISSIONS http://www.sciencemag.org/help/reprints-and-permissions

Use of this article is subject to the Terms of Service

Science (print ISSN 0036-8075; online ISSN 1095-9203) is published by the American Association for the Advancement of Science, 1200 New York Avenue NW, Washington, DC 20005. 2017 © The Authors, some rights reserved; exclusive licensee American Association for the Advancement of Science. No claim to original U.S. Government Works. The title *Science* is a registered trademark of AAAS.

Downloaded from http://science.sciencemag.org/ on December 14, 2017